

FIG. 1. Visualization of string-like segmental cooperative motion in a model glass-forming polymer melt. The monomers that move cooperatively are indicated by the large spheres. Different groups are indicated with different colors. All other polymer segments are shown as translucent thin cylinders.

To clarify the physical nature of the problem and motivate the model for string-like correlated motion, it is helpful to visualize the cooperatively replacing monomers. Figure 1 shows a representative “snapshot” of these replacing mobile particles, which clearly indicates their string-like connectivity. The slender segments in this figure correspond to polymer backbone bonds and the spheres indicate the string-like coordinated particle rearrangement events. The strings shown in Fig. 1 are *equilibrium* structures, and their polymeric form (defined simply as a chain of repeating units) is evident. However, we emphasize that the string-like connectivity refers to the coordinated motion of polymer segments, rather than to the polymer chains having fixed covalent linkages, and thus should not be confused with chain reptation. This type of collective motion is seen in many glass-forming fluids, and so we expect the phenomenon to be a general feature of structural glass-forming liquids.

Since the “strings” are comprised of highly mobile particles, the identity of which vary depending on the time interval  $t$  considered, the strings are themselves highly dynamic objects. This inherently dynamic nature is illustrated in Fig. 2(a), which shows the average  $L(t)$  over the entire  $T$  range studied in the simulations. As discussed in earlier works,<sup>19,20,24–27</sup>  $L(t)$  is small for very short (ballistic) and very long (diffusive) time intervals, when mobility correlations are weak; at intermediate time,  $L(t)$  has a peak, defining the characteristic size  $L$ , at a time that defines the characteristic string “lifetime.” The characteristic  $L$  grows on cooling towards  $T_g$ , as demanded if these objects are identified with the CRR of the AG model. It should be appreciated that this characteristic size (mass) also has an accompanying characteristic spatial extent, the average radius of gyration of these polymeric structures. This string lifetime is approximately proportional to  $t^*$ , the peaking time of the much studied non-Gaussian parameter. Previous work has shown that the lifetime of the strings corresponds to a

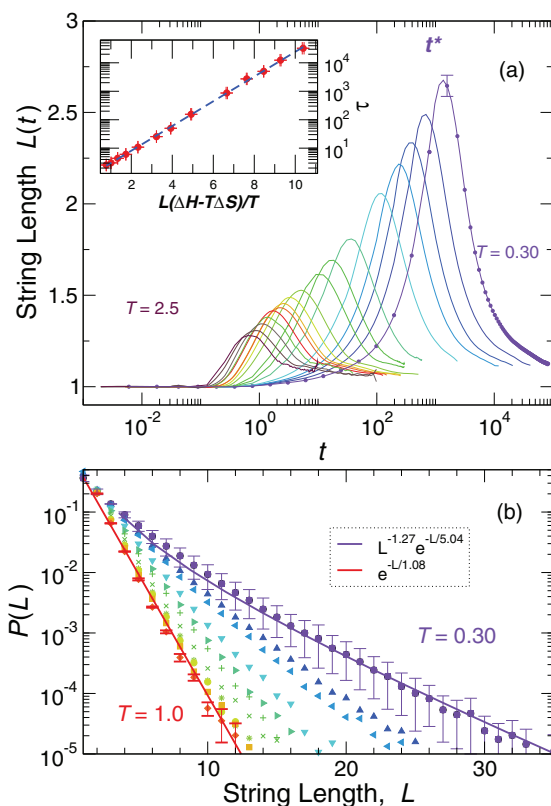


FIG. 2. (a) Average string length  $L(t)$  as a function of interval  $t$  for many  $T$  approaching  $T_g$ . The color gradient indicates  $T$ , from violet at  $T = 0.30$  to maroon at  $T = 2.5$ . The error bars indicate the statistical uncertainty obtained from four independent runs. The inset shows the  $\alpha$ -relaxation time  $\tau$  can be described by the AG relation (Eq. (4)), where the size of the CRR,  $z$ , is exactly identified with string length  $L$ . (b) String length distribution  $P(L)$  at the characteristic peak time  $t^*$  of string size. At high  $T$ ,  $P(L)$  has a nearly exponential form (red line for  $T = 1.0$ ), a canonical property of the linear equilibrium polymers in mean field theory. At low  $T$ , there is curvature in  $P(L)$  that can be approximately captured by a power-law dependence for small  $L$  (violet line at  $T = 0.30$ ), suggesting a possible change in string topology, as discussed in the text.

diffusive relaxation time,<sup>20</sup> so this relaxation time is intermediate between the high frequency beta relaxation regime and the timescale of alpha structural relaxation. Although the strings are related to a diffusive molecular motion, they are linked to  $\alpha$  relaxation at longer times through a power law decoupling relation, which makes the strings relevant to understanding changes of the activation energies governing *both* diffusion and structural relaxation.<sup>19</sup>

In addition to mean string size, it is instructive to examine the distribution of string sizes  $P(L)$  at the characteristic time where  $L(t)$  is largest. If strings can be described as equilibrium polymers, we expect  $P(L)$  to exhibit a nearly exponential mass dependence.<sup>28</sup> Consistent with this expectation, Fig. 2(b) shows that the mass distribution of the strings follows an approximately exponential variation, as noted in previous studies.<sup>20,24</sup> However, at low  $T$ , modest curvature is evident in  $P(L)$  in Fig. 2(b). The deviations from exponential behavior at small  $L$  can be reasonably described by a power-law variation, so that

$$P(L) \sim L^{-\theta} e^{-L/L_0}. \quad (1)$$

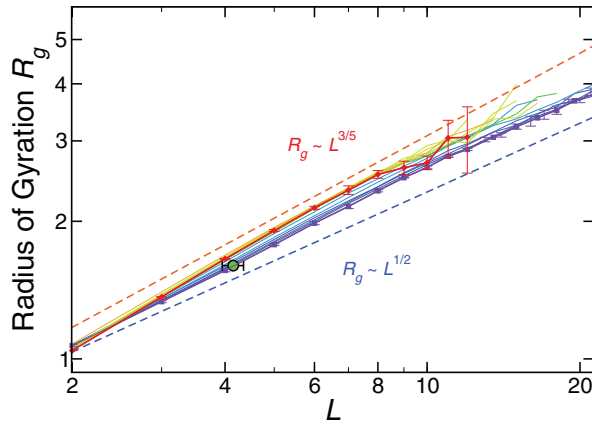


FIG. 3. Dependence of the radius of gyration  $R_g(L)$  on the string length, defining the mass scaling exponent  $\nu$ . The color gradient goes from blue at the lowest  $T = 0.30$  to red at  $T = 1.0$ . The dashed lines indicate the limiting scaling behaviors of the SAW ( $\nu = 3/5$ ) and RW ( $\nu = 1/2$ ). The error bars indicate the statistical uncertainty obtained from four independent runs. The filled green circle indicates the mean estimated value of  $\langle R_g \rangle$  in the low  $T$  limit corresponding to the predicted low  $T$  mean  $L \approx 4.1$  from the string-polymerization model (discussed below).

This type of power law times an exponential scaling for the distribution of replacing particles has recently been seen in simulations of lipid membranes,<sup>29</sup> where  $\theta$  has a similar value. If such a form is used for all  $T$ , we find the exponent  $\theta$  increases on cooling toward  $T_g$ . Interestingly, an exponent value of  $\theta = 2.5$  is consistent with ideal ring equilibrium polymers. Consequently, the increase of  $\theta$  may reflect a progressive topological transition between open strings at high  $T$ , to predominantly ring-like structures at low  $T$ , as seen in crystal melting<sup>30</sup> and the polymerization of dipolar fluids.<sup>31</sup> Regardless of whether such a scenario occurs here, it is apparent that the exponential tail is the predominate feature of our data for  $P(L)$ , a characteristic of equilibrium polymers.

We can further characterize the structure of these strings by their radius of gyration  $R_g$  and its relation to string size,

$$R_g \sim L^\nu, \quad (2)$$

where  $d_f = 1/\nu$  defines the fractal dimension of the strings. For short strings, excluded volume interactions dominate, so strings can be expected to behave like self-avoiding walks (SAW) with  $\nu = 3/5$ . Figure 3 shows that, indeed, such behavior holds, but that  $\nu$  approaches  $1/2$  for longer strings, which occur primarily at low  $T$ . This change can be understood by the proposed analogy to equilibrium polymers. Specifically, the longer the chains grow, the stronger their interchain interactions become, resulting in a greater screening of their excluded volume interactions, just as in ordinary flexible linear equilibrium polymers.<sup>28</sup> This screening causes strings to become progressively more like simple random walks (RW), which have  $\nu = 1/2$ , consistent with the observed behavior.

### III. STRINGS AS COOPERATIVELY REARRANGING REGIONS

A convenient way to parameterize the rapid growth of relaxation time  $\tau$  approaching  $T_g$  is through the effective activation free energy  $\Delta G(T)$ . Assuming that relaxation can be

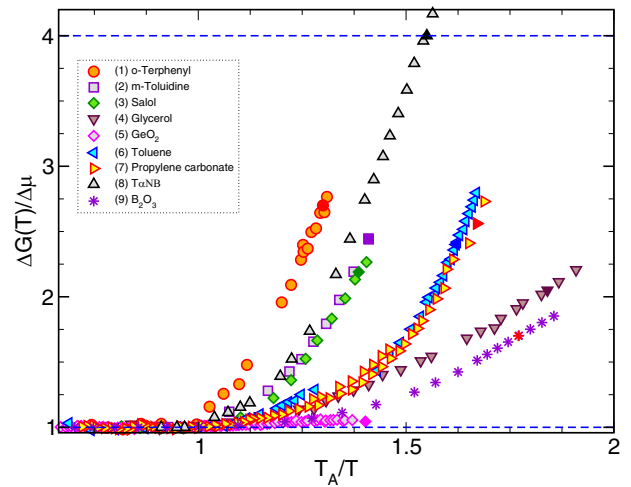


FIG. 4. Temperature dependence of the experimental relative activation energy  $\Delta G(T)/\Delta\mu$  for different glass-forming liquids. The filled symbols with a darker color indicates their values at  $T_g$ . Data were obtained from multiple resources: (1) o-terphenyl Fig. 2 of Ref. 33, (2) m-toluidine from Fig. 8 of Ref. 34, (3) salol from Fig. 3 of Ref. 35, (4) glycerol from Fig. 4 of Ref. 36, (5)  $\text{GeO}_2$  from Fig. 2 of Ref. 33, (6) toluene from Fig. 4 of Ref. 37, (7) propylene carbonate from Fig. 4 of Ref. 38, (8) T $\alpha$ NB Fig. 15 of Ref. 39, (9)  $\text{B}_2\text{O}_3$  from Table 2 of Ref. 40. Note that, while these data are well known, it is the first time that this form of data reduction has been considered. See original references cited above for a discussion of experimental uncertainties for the data shown in this figure.

described as a thermally activated process,  $\Delta G(T)$  can be defined by

$$\Delta G(T) \equiv k_B T \ln(\tau/\tau_0), \quad (3)$$

where  $\tau_0$  is a vibrational relaxation time, approximated as  $\tau_0 \approx 10^{-13}$  s (or  $\tau_0 \approx 0.1$  in our reduced units) for small molecule fluids. Above  $T_A$ ,  $\tau$  has simple Arrhenius dependence,<sup>32</sup> and the activation free energy  $\Delta G(T > T_A) \equiv \Delta\mu$ . As  $T_g$  is approached, the activation free energy  $\Delta G$  grows, but the magnitude of this change is modest. Figure 4 illustrates  $\Delta G(T)/\Delta\mu$  for a number of different GF liquids, where Tri- $\alpha$ -Naphthyl Benzene, T $\alpha$ NB, shows the largest change  $\Delta G(T_g)/\Delta\mu \approx 4$  at  $T_g$  in this collection of GF liquids. The data in this figure are well-known in the glass literature, but, surprisingly, we could not find this data presented in a way that directly indicates the variation of activation free energy. It is striking how small the variation in  $\Delta G(T_g)/\Delta\mu$  needs to be to account the variable relaxation time and fragility of glass-forming liquids.

The approach developed by Adam and Gibbs<sup>6</sup> rationalizes the growth of the activation free energy by hypothesizing that  $\Delta G$  is extensive in the size  $z$  of CRR, so that  $\Delta G = z\Delta\mu$ . Thus, under the assumption of activated dynamics,

$$\tau = \tau_0 \exp[z \Delta\mu/k_B T]. \quad (4)$$

If  $z$  approaches unity at high  $T$ , the limiting Gibbs free energy of activation  $\Delta G = \Delta\mu$ . In their original work, AG assumed (without explanation) that the entropic contribution  $\Delta S_a$  to  $\Delta\mu \equiv \Delta H_a - T\Delta S_a$  could be neglected, so that  $\Delta\mu \approx \Delta H_a$ . When  $z$  is constant (expected at high  $T$ ), this assumption can be justified by a simple redefinition of  $\tau_0$  to incorporate  $\Delta S_a$ ; however, the validity of the assumption is



of the clusters to form smaller chains. Although this model is rather idealized, it has been popular in modeling the formation of worm-like micelles,<sup>51</sup> magnetic chain formation of dipolar particles,<sup>31</sup> protein fiber formation,<sup>52–55</sup> DNA origami tiles,<sup>56</sup> etc.

A well-known result of the FA model is that the average length  $L$  of the dynamic polymer chains at fixed initial concentration of the associating species grows on cooling in a simple Arrhenius fashion,

$$L \simeq L_0 \exp\left(\frac{\Delta H_p}{2k_B T}\right), \quad (6)$$

where  $L_0$  is a constant determined by molecular parameters of the polymerization model and  $\Delta H_p$  is the enthalpy of polymerization. In the FA model, exact calculations dictate  $L = 1$  at high temperatures, corresponding to non-existence of polymeric structures.<sup>57,58</sup> If we formally identify the string size  $L$  with the CRR of AG and adopt the FA model to describe the string formation thermodynamics, Eqs. (4) and (6) imply a “double-exponential”  $T$  dependence of relaxation,

$$\tau = \tau_0 \exp\left[\Delta G_o \exp\left(\frac{\Delta H_p}{2k_B T}\right)\right]. \quad (7)$$

Indeed, such a relation qualitatively captures the very rapid change of relaxation on cooling toward  $T_g$ . In fact, it has been recently noted that Eq. (7) describes the temperature dependence of relaxation times of diverse glass-forming liquids,<sup>59</sup> which we can take as an encouraging sign for modeling strings as equilibrium polymers.

However, our goal is to go beyond curve-fitting relaxation data, and a closer examination of the string data (Fig. 2) reveals a significant problem with applying the FA model (and consequently Eq. (7)); namely, the average polymerization index  $L$  does not approach 1 at high  $T$ , which is demanded in the FA model. Instead,  $L$  takes a somewhat larger value,  $L(T_A) \equiv L_A \approx 1.4$  (see Fig. 2). The intuitive assumption that cooperative motion is completely absent at high  $T$  would lead us to expect, as suggested by AG, that the extent  $L \rightarrow 1$  at high  $T$ , but apparently, some cooperativity remains at elevated temperatures.<sup>60</sup> Since the string sizes are exponentially distributed (Fig. 2(b)), a mean size of 1.4 implies that there much larger strings in the system. This may seem like a small effect, but a change in the mean string length by 0.4 implies an appreciable change in the dynamics of the fluid. Of the many models of equilibrium polymerization, we know only one analytically tractable model that has the property that the average degree of polymerization  $L$  does not approach unity upon heating.<sup>28,61</sup> In this “living polymerization model,” a distinct species having a fixed concentration serves to initiate the polymerization process. The thermally activated polymerization theory is a plausible model for glass-forming liquids, and there is precedent for inferring thermally activated excitations that influence molecular transport through initiation of collective molecular motion. For example, unstable five-coordinated molecules in water have been shown to “catalyze” molecular motion in water.<sup>62,63</sup> Granato and co-workers have similarly argued that relatively *high density* interstitial excitations exist in liquids and glasses,<sup>64</sup> and they rationalized many of the low temperature properties of

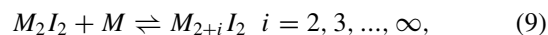
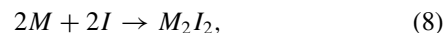
condensed disordered materials based on this model.<sup>65</sup> Keys *et al.*<sup>66</sup> have identified thermally activated elementary excitations that seem to be associated with string-like collective motion. In future work, we hope to find a quantitative relation between these high frequency excitations and those studied in the present work. The physical nature of activating molecules also requires an in depth investigation.

Based on these considerations, we next test the extent to which the strings in our glass-forming liquid can be quantitatively described by living polymerization. In the comparison of the model to our molecular simulations, we consider multiple thermodynamic properties to ensure self-consistently. After establishing this consistency, we then examine the implications of our polymerization model for predicting the properties of our glass-forming liquid outside the temperature range in which equilibrium simulation is possible. We find that this model makes valuable predictions about the nature of the glass state and the general nature of the glass transition.

## B. Living polymerization model of strings

In order to explain the  $T$  dependence of the strings, and thus of  $\Delta G$ , we now consider the theoretical implications of the hypothesis that these strings can be considered as dynamic polymers that form and disintegrate in equilibrium.

We consider a model for initiated equilibrium polymerization by Dudowicz *et al.*,<sup>28</sup> which assumes that chain formation is governed by two simple reactions:



where reaction of the monomer species  $M$ , mobile particles in the context of glass-forming liquids, requires an energetically excited initiating species  $I$ . Such energetically activated particles are exemplified in water by the occurrence of local high density configurations which catalyze molecular movement.<sup>62,63,67</sup> The strings are dynamic polymers of these highly mobile monomers that have a temperature dependent average length, or polymerization index,  $L \equiv \langle L \rangle$ . The dynamics polymer should not be confused with the covalently bonded polymer chains. The fraction of linked mobile particles  $\Phi$  serves as the order parameter for the string self-assembly process, and  $L$  and  $\Phi$  of living polymer solutions are related by

$$L = \frac{1}{1 - \Phi + r/2}, \quad (10)$$

where  $r$  is the ratio of the initiator to the monomer volume fraction  $\phi_0$ .  $\Phi$  is limited to the range  $r \leq \Phi \leq 1$ . Consequently,  $L$  has an upper bound determined by  $r$ , a fact that has important implications for glass formation at low  $T$ . Note that the high temperature limit of  $L$  (where  $\Phi \approx r$ ) from Eq. (10) is larger than 1, consistent with our MD simulations observations on GF liquids.

To test the applicability of this model of string formation for GF fluids, we need to map observable quantities from the simulation to the input variables of the theory. For initiated,

or “living” polymerization,  $r \approx \Phi$  for  $T$  above the “onset” temperature in the theory (see Fig. 7 of Ref. 28). Similarly, we know that string-like motion in GF liquids is only prevalent below an onset temperature  $T_A$  where relaxation becomes non-Arrhenius and caging becomes conspicuous.<sup>32,68</sup> Thus, we restrict the application of the polymerization model to  $T \lesssim T_A$ . Identifying the onset condition in the simulation and in living polymers, we have  $L(T_A) \equiv L_A$ . The approximations  $r \approx \Phi_A$  and Eq. (10) give rise to the useful closed analytic form,

$$L \approx \frac{L_A \left(1 - \frac{\Phi_A}{2}\right)}{1 - \Phi + \frac{\Phi_A}{2}}, \quad T \leq T_A, \quad (11)$$

expressed in terms of observable properties,  $L_A$ ,  $\Phi_A$ ,  $\Phi$ . In the living polymerization model,  $L_A$  and  $\Phi_A$  are not independent, but we take these as independent observables in our application of Eq. (11) because of the approximation  $\Phi_A \approx r$ . Equations (10) and (11) imply that  $L$  saturates to a constant value at low  $T$ , a point extensively discussed below. In living polymer solutions, the magnitude of  $r$  (and thus  $\Phi_A$  by analogy) links the string mass at high and low  $T$  and also governs the cooperativity of the polymerization transition,<sup>69</sup> as measured by the rate of change of  $L(T)$ , and the magnitude of the change in the specific heat; similar definitions of cooperativity have been applied to GF liquids.<sup>19,70</sup>

In the living polymerization model, the order parameter  $\Phi$  is the extent of polymerization, defined by the fraction of monomers forming polymeric structures. In our case, this is the fraction of those highly mobile monomers participating in strings, and Fig. 6 shows the temperature dependence of  $\Phi(T)$ . We find that the variation of the behavior of  $\Phi(T)$  is well described by the polymerization model prediction,<sup>28</sup>

$$\Phi = 1 - \phi(T)/\phi_0, \quad (12)$$

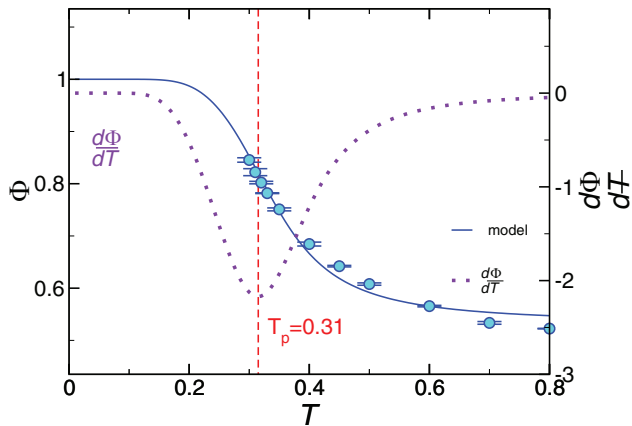


FIG. 6. Temperature dependence of the extent of polymerization  $\Phi(T)$ . The symbols represent the simulation data. The solid curve represents the model prediction for  $\Phi$ . The dashed curve illustrates the numerical derivative of  $\Phi(T)$ . The minimum of  $\frac{d\Phi}{dT}$  defines the polymerization transition location  $T_p$ , indicated by the vertical line. The error bars indicate the statistical uncertainty obtained from four independent runs.

where  $\phi(T)$  is the fraction of monomers, given by<sup>28</sup>

$$\phi(T) = \frac{1}{2} e^{\frac{\Delta G_p}{k_B T}} \left[ 1 + \phi_0 \left( 1 - \frac{\Phi_A}{2} \right) e^{-\frac{\Delta G_p}{k_B T}} - \sqrt{\left( 1 + \phi_0 \left( 1 - \frac{\Phi_A}{2} \right) e^{-\frac{\Delta G_p}{k_B T}} \right)^2 - 4\phi_0(1 - \Phi_A)e^{-\frac{\Delta G_p}{k_B T}}} \right]. \quad (13)$$

The free energy  $\Delta G_p = H_p - T\Delta S_p$  describes the thermodynamics of polymerization (string formation) where  $\Delta H_p$  and  $\Delta S_p$  are the enthalpy and entropy of chain assembly, respectively. Note that the free energy of polymerization  $\Delta G_p$  should not be confused with the system activation free energy  $\Delta\mu$  (and similarly for enthalpy and entropy). Accordingly, the association into a strings is governed by an equilibrium constant  $k = \exp[\Delta G_p/k_B T]$ . The volume fraction of mobile particles  $\phi_0 = f_0(\pi/6) = 0.034$ , using a mobile particle fraction  $f_0 = 0.065$ , determined in earlier work.<sup>71</sup>

We next test the validity of the relation between  $L$  and  $\Phi$  (Eq. (11)) in Fig. 7(a) using *no fitting parameters*, since  $L_A$ ,  $\Phi_A$  are taken directly from the numerical results. The figure shows agreement over the entire range of temperature investigated. We note that the  $\Phi_A = 0.52$ , which may seem large at first glance. However, recall that this is the fraction of the relatively small subset of mobile particles so that the initiator volume fraction  $\phi_I = 0.018$  is quite small. Moreover, Ref. 30 found that the mobile particles associated with the “activated” species have a concentration that is comparable to the coordination number of the mobile particles. This rough argument

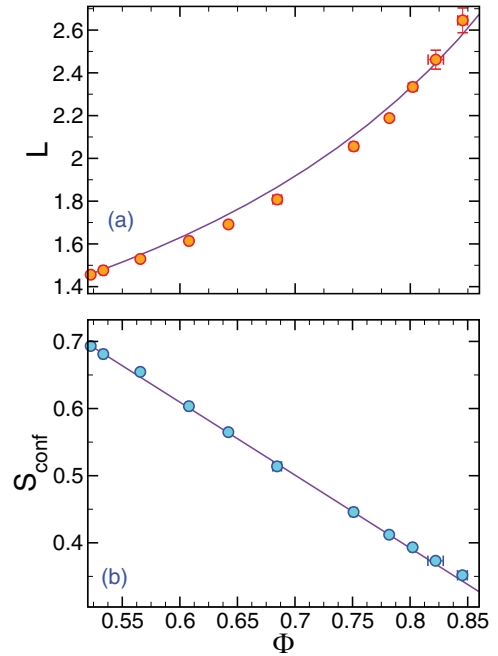


FIG. 7. (a) Model prediction of the string mass  $L$  as a function of the fraction  $\Phi$  of mobile-particles in the strings. Simulation results are given by the solid symbols, and the solid curve represents Eq. (11) with no free parameters. (b) Test of the living polymerization model relationship between the configurational entropy  $S_{\text{conf}}$  and  $\Phi$ . We find excellent agreement with the predicted linear relation,  $S_{\text{conf}} \propto (1 - \Phi)$ . Note that, in the free association model of self-assembly,<sup>70</sup>  $S_{\text{conf}} \propto (1 - \Phi)^{1/2}$ , providing further evidence of the inadequacy of the FA model in describing glass formation.

makes the activated particles on the order of 50%, as we find here. In both the AG and living polymerization models, the activation energy is expected to vary inversely proportional to the configurational entropy  $S_{\text{conf}}$ .<sup>28,70</sup> Since  $L$  also varies inversely to  $\Phi$ , we then expect  $S_{\text{conf}} \propto (1 - \Phi)$ . Figure 4(b) confirms this expectation, providing a possible alternative means of estimating  $S_{\text{conf}}$ , a quantity highly cumbersome to compute in molecular simulations. Notably, there are also fundamental experimental difficulties in estimating  $S_{\text{conf}}$ . It is not possible to reliably experimentally estimate from specific heat measurements, as AG originally suggested, because  $S_{\text{conf}}$  can be quite small in comparison with the vibrational entropy in polymer fluids.<sup>20</sup>

Given the success of this initial parameter-free test on the string model for glass-formation, we next consider the implications of this theoretical description for the  $T$  dependence of  $L(T)$ , and thus  $\tau(T)$ , both in the region where we have simulation results, and also at lower  $T$ , approaching  $T_g$  and below.

Using the living polymerization model prediction for the  $T$  dependence of  $\Phi(T)$ , we obtain an analytic expression for  $L(T)$  using Eq. (13) in Eq. (11) (which we do not list, for brevity). In addition, we may obtain a simpler expression by combining Eq. (11) and the high  $T$  expansion of  $\Phi$  from Ref. 28, which yields the approximate high  $T$  expansion,

$$L \approx L_A \left(1 - \frac{\Phi_A}{2}\right) \left[1 + \frac{\Phi_A}{2} \left(1 + \phi_0 \exp\left[-\frac{\Delta G_p}{k_B T}\right]\right)\right], \quad (14)$$

which exhibits the expected Arrhenius  $T$  dependence of  $L$  for equilibrium polymerization models at high  $T$ . We expect Eq. (14) to be valid in the range  $T_c \lesssim T \lesssim T_A$ , where  $T_c$  is the crossover temperature frequently associated with the mode-coupling theory of supercooled liquid dynamics.<sup>72</sup> In practice,  $T_c$  is obtained by empirically fitting  $\tau$  to a power-law in  $T - T_c$  over a restricted  $T$  range and, in the present work,  $T_c = 0.35$ .<sup>20</sup> The polymerization temperature  $T_p$  indicated in Fig. 6 is defined by the temperature at which  $\partial\Phi/\partial T$  reaches its minimum,  $T_p = 0.31$ . Since  $T_p$  is an intermediate temperature, it is natural to consider its possible relation to  $T_c$  of glass formation. Ref. 70 argued that  $T_c$  should be identified with  $T_p$  in the polymerization model, and our  $T_c$  value is in reasonable accord with our estimate of  $T_p$ .

The  $T$  dependence of  $L$  predicted by the full theory, as well as the high  $T$  approximation are shown in Fig. 8, where  $\Delta H_p = -1.55$  and  $\Delta S_p/k_B = -0.46$ . Both the complete expression and high  $T$  expansion can account for the  $T$  dependence of the available data for  $L$ , but show dramatically different behavior when we extend to lower  $T$ . The high  $T$  expansion predicts unbounded string growth ( $L \rightarrow \infty$ ), but the nature of the high  $T$  approximations make this estimate unreliable at low  $T$ . In contrast, the complete model (without approximation) predicts that  $L(T)$  reaches a plateau at low  $T$ ,  $L(T \rightarrow 0) = L_A(\frac{2}{\Phi_A} - 1) \approx 4.1$ , corresponding to a radius of gyration  $R_g = \sqrt{L} \approx 1.6 \sigma \approx 1.6 \text{ nm}$  to  $3.2 \text{ nm}$  (see Fig. 3). This length scale is consistent with empirical CRR size estimates obtained from specific heat measurements in small-molecule liquids and estimates of the change in the activation energy in GF liquids.<sup>40,73,74</sup> This range of length scales

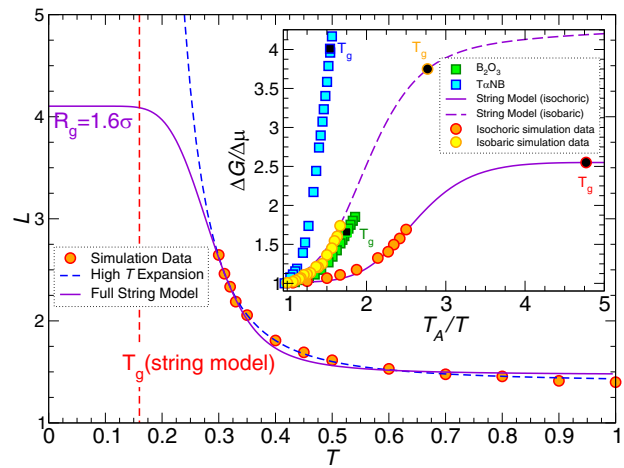


FIG. 8. Temperature dependence of the string length  $L(T)$ . The lines in main panel represent the model predictions from the full theory (solid line) and the high  $T$  expansion (dashed line). The full theory reaches a plateau at low  $T$ , while the high  $T$  approximation yields a divergence. (Inset) The comparison of  $\Delta G/\Delta\mu$  for simulation data and  $\Delta G/\Delta\mu$  for the experimental values (which should equal  $L/L_A$  to our simulation data of our glass former model). The experimental data emphasize the similarity to our simulation data. We compare the equilibrium polymer model data both isobaric and isochoric simulation data to show that change does not alter the qualitative trend. Note the somewhat stronger  $T$  variation of the reduced activation energy  $\Delta G/\Delta\mu$ , and thus, fragility in the constant pressure simulations. McKenna and co-workers<sup>76</sup> have also found the  $T$  dependence of the structural relaxation measurements on polymeric glass-forming liquids to be weaker under constant density conditions.

also accords with the typical “cooperative motion scale” from neutron and Raman scattering, Boson peak, and NMR measurements.<sup>75</sup> In addition, the inset of Fig. 8 shows that the predicted low  $T$  limit of  $\Delta G/\Delta\mu = L/L_A$  from our model is compatible with the experimentally observed behavior of several glass-forming liquids.

Using the AG-inspired relation,  $\Delta G(T) = (\Delta H_a - T\Delta S_a)L(T)/L_A$ , we obtain our string model for  $\tau(T)$ ,

$$\tau(T) = \tau_0 \exp[(\Delta H_a - T\Delta S_a)(L(T)/L_A)/k_B T], \quad (15)$$

to predict the the structural relaxation time at  $T$  lower than those accessible by equilibrium simulation (Fig. 9(a)). First, we note that using either the high  $T$  approximation or the full model for  $L$  accounts well for  $\tau$  in the  $T$  range where simulation data are available. However, the behavior of the full and approximate model differ significantly at lower  $T$ . The predicted behavior for  $\tau(T)$  can be compared with that obtained from the commonly used Vogel-Fulcher-Tammann (VFT) equation,<sup>77–79</sup>

$$\tau_\alpha = \tau_0 \exp\left[\frac{DT_0}{T - T_0}\right], \quad (16)$$

where, for the present data,  $T_0 = 0.20$ <sup>20</sup> is the extrapolated divergence temperature of  $\tau$ . Interestingly, the fit using the VFT form is nearly indistinguishable from the extrapolation of the high  $T$  approximation to the string model. Both show a more rapid predicted growth of  $\tau$  at low  $T$  than that of the full string model. One way to quantify this difference is in terms of  $T_g$ . Using the common laboratory definition of  $T_g$  as  $\tau(T_g) \approx 100s$ , and taking our reduced time unit as 1 ps, we find from the string model  $T_g = 0.16$ . Due to the more rapid variation



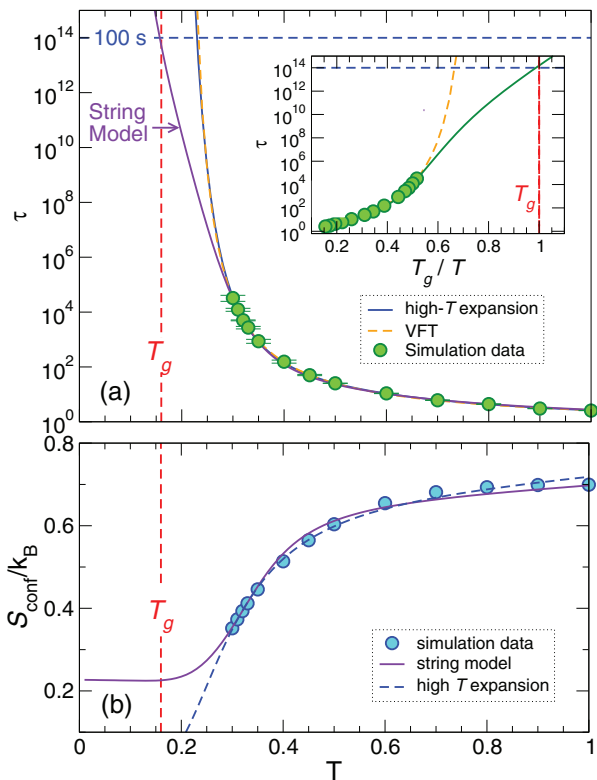


FIG. 9. (a) Temperature dependence of  $\tau(T)$  and the prediction for  $\tau$  from combining the string model with the AG expression (Eq. (15)). We also show the fits to the VFT equation, as well as the high- $T$  expansion of the string model. Note that for the high- $T$  expansion is nearly coincident with the VFT extrapolation. The horizontal dashed blue line illustrates the value where  $\tau \approx 100$  s, which typically defines the glass transition temperature. The inset shows  $\tau$  as a function of  $T_g/T$  in order to highlight the predicted return to Arrhenius (strong) behavior in the vicinity of  $T_g$ . (b) Configurational entropy  $S_{\text{conf}}(T)$  from numerical simulations<sup>20</sup> in comparison with the predicted variation from the string model.

of the high  $T$  approximation and the VFT fit, the estimated  $T_g(\text{VFT}) = 0.23$  is larger than predicted from the full string model described in the present paper. This large discrepancy in  $T_g$  estimates is primarily a consequence of the fact that  $L$  approaches a constant at low  $T$  in the string model.

The plateau of  $L(T)$  at low  $T$  has important consequences for the low  $T$  behavior of  $\tau$ . Specifically, such a plateau implies a return to an Arrhenius temperature dependence, as illustrated in the inset of Fig. 9(a). Consequently, the fragility, based on the string model, is smaller than values estimated from a VFT fit. This “fragile-to-strong” crossover in the string model occurs rather close to the expected  $T_g$  for the system. Given the extrapolation required to assign a precise value for  $T_g$ , it is plausible that this crossover behavior occurs roughly on entering the glass state. Such an Arrhenius temperature dependence near  $T_g$  has been observed in a variety of GF fluids,<sup>1</sup> and recent experimental aging results in a 20 million-year-old amber suggests this Arrhenius behavior continues significantly below  $T_g$ ,<sup>80</sup> as the our polymerization model predicts.

Based on the inverse scaling relation between  $L$  and  $S_{\text{conf}}$ , we can also use  $L$  from the polymerization model to anticipate the low  $T$  behavior of  $S_{\text{conf}}$ , shown in Fig. 9(b). Configurational entropy is taken from Ref. 28, and the  $T$  dependence of  $S_{\text{conf}}$  is similar to that of many fluids.<sup>9–16,81</sup>

The low  $T$  plateau of  $L$  corresponds to a prediction for the saturation of  $S_{\text{conf}}$  to a residual low  $T$  residual value that is about one-quarter of its value near  $T_A$ . Consequently, the Kauzmann entropy “catastrophe,”<sup>1</sup> in which  $S_{\text{conf}}$  would be negative at low  $T$ , is naturally avoided in the string model of glass formation. The plateau in  $S_{\text{conf}}$  does not violate any thermodynamic relationship, and there is experimental evidence<sup>82</sup> that the predicted plateau in  $S_{\text{conf}}$  at low  $T$ , accompanying the plateau in  $L$ , can occur as an *equilibrium* phenomena. For example, the X-Y spin model can be described by equilibrium polymerization transition involving directed closed strings (rings).  $S_{\text{conf}}$  remains constant in this model for a substantial  $T$  range at low  $T$ , as in our string model of glass-forming liquids.<sup>83</sup>

The residual entropy as  $T$  approaches zero is determined by  $\Phi_A$  and  $L_A$  in the living polymerization model, and these parameters control the sharpness or “cooperativity” of the polymerization transition. If we consider the extrapolation of the high  $T$  expansion to estimate  $S_{\text{conf}}$  at low  $T$  (Fig. 9(b)), we see the extrapolation predicts a Kauzmann temperature  $T_k = 0.2$  (i.e., where  $S_{\text{conf}} = 0$ ). The vanishing is an artifact of the high- $T$  expansion, and the data are entirely consistent with an earlier extrapolation of  $S_{\text{conf}}$  based on a simple polynomial fit,<sup>20</sup> as well as the VFT extrapolated divergence temperature  $T_0$ . A similar vanishing of  $S_{\text{conf}}$  based on the use of a high  $T$  expansion outside its range of validity is also found in a recent entropy theory for polymer glass formation.<sup>84</sup> Although the vanishing of  $S_{\text{conf}}$  here is a result of an improper extrapolation, the VFT and Kauzmann temperatures remain useful characterization temperatures of glass formation. The temperature is at least better defined than  $T_g$ , whose value varies appreciably with cooling rate.

## V. CONCLUSIONS

Our identification of the living polymerization model with clusters of coherent string-like displacements in GF liquids implies that glass formation can be interpreted as a kind order-disorder transition in which particles reversibly associate into string-like clusters at equilibrium, but where the “polymerized” ordered state that does not have long-ranged translational order. This type of order-disorder, or “rounded” transition,<sup>85</sup> is accompanied by progressive, but continuous, changes in enthalpy and configurational entropy and is characteristic of numerous self-assembly process in nature. Since rounded transitions are not phase transitions having a well-defined critical temperature, it is necessary to characterize these relatively broad transitions with an onset temperature  $T_A$ , and end-point temperature, here  $T_g$  (or perhaps better,  $T_0$ ). In living polymerization, the approximate midpoint  $T$  is termed the polymerization temperature,  $T_p$ .

Dynamical heterogeneity in the form of strings seems to be ubiquitous in strongly-interacting, condensed-phase systems, ranging from simple GF fluids, to the interfacial dynamics of nanoparticles, lipid membranes, crystal melting, and grain boundaries,<sup>24,29,30,86–88</sup> and may be relevant to describe physical aging in glass-forming liquids.<sup>89</sup> Strings have been observed directly experimentally in the amorphous interfacial region of crystals and in particle tracking

measurements of granular and colloidal particles.<sup>90,91</sup> Such string-like excitations are natural expressions of thermal fluctuations associated with the progressive emergence of rigidity in cooled liquids, and equilibrium polymerization models have been introduced to describe emergent collective macroscopic response in other contexts.<sup>92</sup> For example, polymerization models have been used to describe the disorder transition in type II superconductors<sup>93</sup> and the melting transition of crystals.<sup>94</sup> In modeling the heterogenous nature of turbulent fluids, the vortex fluid excitations have been modeled as equilibrium polymers.<sup>95</sup> Zwanzig<sup>96</sup> developed a theory of elementary excitations in classical liquids that parallels the treatment of collective excitations in liquid <sup>4</sup>He, and this framework offers a potential starting point for understanding the strings at a more fundamental level.

Keys *et al.*<sup>66</sup> have also introduced a thermal excitation model of glass-forming liquids that might have some relation to those in our work, but there are qualitative differences in the character of these excitations from those studied in the present work. While their excitations are likewise associated with persistent changes in particle displacement, their size exhibits essentially no temperature dependence and their concentration changes with temperature, features different from strings whose average length  $L$  is directly related to the activation energy of structural relaxation and diffusion. There is no real discrepancy. Since the collective excitations of Keys *et al.*<sup>66</sup> occur on a picosecond timescale rather than the string lifetime, which relates to relaxation time related to molecular diffusion. As Keys *et al.* note, their excitations are more closely related to the microstrings<sup>66</sup> (or stringlets<sup>97,98</sup>) defined in previous work on glass-forming liquids, and future work should investigate the relation between these fundamentally different thermal excitations. The facilitation approach to glass formation<sup>66</sup> is also predicated on a different physical view of glass formation. This approach is built around a purely dynamical description of vitrification, while our approach, like that of the Adam-Gibbs theory and the RFOT, are founded on an intimate linkage between thermodynamics and dynamics.

Finally, we make some general observations about our modeling of structural relaxation in relation to the classical Adam-Gibbs model.<sup>6</sup> The string model of glass-formation involves a number of extensions and revisions of the AG model:

- AG do not specify the hypothetical forms of their clusters. Our theory indicates these CRR have the form of self-avoiding polymers with progressively screened excluded volume interactions upon cooling. The string model takes the activation free energy to be proportional to the average string length,  $L$ , a quantity that can be readily identified and computed. We also note that  $L_A$  is larger than unity, a finding having ramifications for our model of relaxation.
- AG assume that  $\Delta\mu$  is a purely temperature independent enthalpic parameter; we include the sometimes appreciable entropy of activation, so that  $\Delta\mu = \Delta H_a - T\Delta S_a$ .
- AG argued that the hypothetical CRR should be weakly interacting to rationalize an inverse scaling be-

tween  $z^*$  and the fluid configurational entropy  $S_{\text{conf}}$ . Instead, the inverse relation between  $L$  and  $S_{\text{conf}}$  naturally derives from the theory of living polymerization. Our simulations show that the string excitations actually exhibit rather strong interactions, leading to a screening of their excluded volume interactions as they grow and interpenetrate.

Our integration of the AG and living polymerization theories evidently involves features that are distinct from AG, even if it is built on the same qualitative picture that the activation free energy varies with the growth of fluid excitations whose mass grows upon cooling. In contrast, the string theory of relaxation offers a quantitative and physically verifiable route to describe the structural nature of cooperative motion in condensed materials, and also provides direct insight into how these structures influence the relaxation and diffusion of the fluid. Of course, this model requires further tests for other glass-forming systems to check its general validity and to better understand the energetic parameters of the theory. An important aspect of this theory is that it provides a metrology for characterizing essential activation parameters and measures of collective motion and fragility that can be widely used to characterize diverse glass-forming materials in materials science and biology.

<sup>1</sup>P. G. Debenedetti, *Metastable Liquids* (Princeton University Press, Princeton, 1996).

<sup>2</sup>M. D. Ediger, *Annu. Rev. Phys. Chem.* **51**, 99 (2000).

<sup>3</sup>R. Richert, *J. Phys.: Condens. Matter* **14**, R703 (2002).

<sup>4</sup>W. Kob, C. Donati, S. J. Plimpton, P. H. Poole, and S. C. Glotzer, *Phys. Rev. Lett.* **79**, 2827 (1997).

<sup>5</sup>T. Kawasaki and H. Tanaka, *J. Phys.: Condens. Matter* **22**, 232102 (2010).

<sup>6</sup>G. Adam and J. H. Gibbs, *J. Chem. Phys.* **43**, 139 (1965).

<sup>7</sup>R. Richert and C. A. Angell, *J. Chem. Phys.* **108**, 9016 (1998).

<sup>8</sup>C. M. Roland, S. Capaccioli, M. Lucchesi, and R. Casalini, *J. Chem. Phys.* **120**, 10640 (2004).

<sup>9</sup>F. Sciortino, W. Kob, and P. Tartaglia, *Phys. Rev. Lett.* **83**, 3214 (1999).

<sup>10</sup>S. Sastry, *Nature* **409**, 164 (2001).

<sup>11</sup>R. J. Speedy, *J. Chem. Phys.* **110**, 4559 (1999).

<sup>12</sup>R. J. Speedy, *J. Chem. Phys.* **114**, 9069 (2001).

<sup>13</sup>L. Angelani and G. Foffi, *J. Phys.: Condens. Matter* **19**, 256207 (2007).

<sup>14</sup>F. W. Starr, S. Sastry, E. La Nave, A. Scala, H. E. Stanley, and F. Sciortino, *Phys. Rev. E* **63**, 041201 (2001).

<sup>15</sup>I. Saika-Voivod, F. Sciortino, and P. H. Poole, *Phys. Rev. E* **69**, 041503 (2004).

<sup>16</sup>S. Mossa, E. La Nave, H. E. Stanley, C. Donati, F. Sciortino, and P. Tartaglia, *Phys. Rev. E* **65**, 041205 (2002).

<sup>17</sup>T. R. Kirkpatrick, D. Thirumalai, and P. G. Wolynes, *Phys. Rev. A* **40**, 1045 (1989).

<sup>18</sup>Y. Gebremichael, M. Vogel, M. N. J. Bergroth, F. W. Starr, and S. C. Glotzer, *J. Phys. Chem. B* **109**, 15068 (2005).

<sup>19</sup>F. W. Starr and J. F. Douglas, *Phys. Rev. Lett.* **106**, 115702 (2011).

<sup>20</sup>F. W. Starr, J. F. Douglas, and S. Sastry, *J. Chem. Phys.* **138**, 12A541 (2013).

<sup>21</sup>B. A. Pazmiño Betancourt, J. F. Douglas, and F. W. Starr, *Soft Matter* **9**, 241 (2013).

<sup>22</sup>P. Z. Hanakata, J. F. Douglas, and F. W. Starr, *J. Chem. Phys.* **137**, 244901 (2012).

<sup>23</sup>G. S. Grest and K. Kremer, *Phys. Rev. A* **33**, 3628 (1986).

<sup>24</sup>C. Donati, J. F. Douglas, W. Kob, S. J. Plimpton, P. H. Poole, and S. C. Glotzer, *Phys. Rev. Lett.* **80**, 2338 (1998).

<sup>25</sup>M. Aichele, Y. Gebremichael, F. W. Starr, J. Baschnagel, and S. C. Glotzer, *J. Chem. Phys.* **119**, 5290 (2003).

<sup>26</sup>C. Donati, S. C. Glotzer, P. H. Poole, W. Kob, and S. J. Plimpton, *Phys. Rev. E* **60**, 3107 (1999).

<sup>27</sup>Y. Gebremichael, M. Vogel, and S. Glotzer, *J. Chem. Phys.* **120**, 4415 (2004).

- <sup>28</sup>J. Dudowicz, K. F. Freed, and J. F. Douglas, *J. Chem. Phys.* **111**, 7116 (1999).
- <sup>29</sup>F. W. Starr, B. Hartmann, and J. F. Douglas, *Soft Matter* **10**, 3036 (2014).
- <sup>30</sup>H. Zhang, M. Khalkhali, Q. Liu, and J. F. Douglas, *J. Chem. Phys.* **138**, 12A538 (2013).
- <sup>31</sup>K. Van Workum and J. F. Douglas, *Phys. Rev. E* **71**, 031502 (2005).
- <sup>32</sup>See supplementary material at <http://dx.doi.org/10.1063/1.4878502> for a description of the evaluation of  $T_A$  and the importance of its value for our analysis.
- <sup>33</sup>D. Kivelson and G. Tarjus, *J. Non-Cryst. Solids* **235–237**, 86 (1998).
- <sup>34</sup>M. Cutroni, A. Mandanici, A. Spanoudaki, and R. Pelster, *J. Chem. Phys.* **114**, 7118 (2001).
- <sup>35</sup>P. K. Dixon, *Phys. Rev. B* **42**, 8179 (1990).
- <sup>36</sup>P. Lunkenheimer, R. Wehn, U. Schneider, and A. Loidl, *Phys. Rev. Lett.* **95**, 055702 (2005).
- <sup>37</sup>A. Döb, G. Hinze, B. Schiener, J. Hemberger, R. Böhmer, G. Hinze, and R. Bo, *J. Chem. Phys.* **107**, 1740 (1997).
- <sup>38</sup>F. Stickel, E. W. Fischer, and R. Richert, *J. Chem. Phys.* **104**, 2043 (1996).
- <sup>39</sup>D. J. Plazek and J. H. Magill, *J. Chem. Phys.* **45**, 3038 (1966).
- <sup>40</sup>P. B. Macedo and A. Napolitano, *J. Chem. Phys.* **49**, 1887 (1968).
- <sup>41</sup>D. Tabor, *Philos. Mag. A* **57**, 217 (1988).
- <sup>42</sup>A. Bondi, *J. Chem. Phys.* **14**, 591 (1946).
- <sup>43</sup>A. B. Bestul and S. S. Chang, *J. Chem. Phys.* **40**, 3731 (1964).
- <sup>44</sup>S. Takahara, O. Yamamuro, and H. Suga, *J. Non-Cryst. Solids* **171**, 259 (1994).
- <sup>45</sup>J. R. Errington, T. M. Truskett, and J. Mittal, *J. Chem. Phys.* **125**, 244502 (2006).
- <sup>46</sup>J. C. Dyre, T. Hechsher, and K. Niss, *J. Non-Cryst. Solids* **355**, 624 (2009).
- <sup>47</sup>N. Gnan, T. B. Schröder, U. R. Pedersen, N. P. Bailey, and J. C. Dyre, *J. Chem. Phys.* **131**, 234504 (2009).
- <sup>48</sup>S. C. Greer, *Annu. Rev. Phys. Chem.* **53**, 173 (2002).
- <sup>49</sup>J. F. Douglas, J. Dudowicz, and K. F. Freed, *J. Chem. Phys.* **128**, 224901 (2008).
- <sup>50</sup>J. Dudowicz, K. F. Freed, and J. F. Douglas, *J. Chem. Phys.* **119**, 12645 (2003).
- <sup>51</sup>H. Wennerstrom and B. Lindman, *Phys. Rep.* **52**, 1 (1979).
- <sup>52</sup>L. Rothfield, S. Justice, and J. Garcia-Lara, *Annu. Rev. Genet.* **33**, 423 (1999).
- <sup>53</sup>G. Lan, A. Dajkovic, D. Wirtz, and S. X. Sun, *Biophys. J.* **95**, 4045 (2008).
- <sup>54</sup>I. Inoue, R. Ino, and A. Nishimura, *Genes Cells* **14**, 435 (2009).
- <sup>55</sup>Y. C. Kim, R. B. Best, and J. Mittal, *J. Chem. Phys.* **133**, 205101 (2010).
- <sup>56</sup>A. Ekani-Nkodo, A. Kumar, and D. K. Fyngenson, *Phys. Rev. Lett.* **93**, 268301 (2004).
- <sup>57</sup>The exact expression for  $L$  in the FA model from a Flory-Huggins lattice model calculation is more complicated<sup>50</sup> than the often reported scaling of Eq. (6). The simpler form is deduced from a continuum formulation of the lattice model.<sup>58</sup>
- <sup>58</sup>M. E. Cates and S. J. Candau, *J. Phys.: Condens. Matter* **2**, 6869 (1990).
- <sup>59</sup>J. C. Mauro, Y. Yue, A. J. Ellison, P. K. Gupta, and D. C. Allan, *Proc. Natl. Acad. Sci. U.S.A.* **106**, 19780 (2009).
- <sup>60</sup>Note that a cooperativity size larger than one at high  $T$  does not affect the expected Arrhenius dependence within the AG approach, since an Arrhenius temperature dependence is recovered, provided that  $L$  becomes nearly constant at high  $T$ . In principle, relaxation can even be Arrhenius when the molecular motion is highly cooperative, provided  $L$  is unchanging with  $T$ . This behavior can also arise at low  $T$ , and we shall see that our living polymerization model in fact predicts that  $L$  saturates to a finite value at low  $T$ , implying a return to an Arrhenius relaxation in the glass state.
- <sup>61</sup>Although it is not apparent from the approximate expression for  $L$  in Eq. (6),  $L$  in the FA model rapidly approaches 1 at high  $T$ , regardless of the concentration of the associating species.
- <sup>62</sup>F. Sciortino, A. Geiger, and H. E. Stanley, *J. Chem. Phys.* **96**, 3857 (1992).
- <sup>63</sup>F. Sciortino, A. Geiger, and H. E. Stanley, *Nature* **354**, 218 (1991).
- <sup>64</sup>A. Granato, *Metall. Mater. Trans. A* **29**, 1837 (1998).
- <sup>65</sup>Granato<sup>64</sup> has estimated that the fraction of interstitially excited atoms in a fluid should be on the order of 2 percent, consistent within our computational uncertainty of our estimate of the initiator concentration. Zhang and Douglas<sup>30</sup> examined the role of interstitial defects in homogeneous crystal melting where it was found that these defects actually drive string-like collective motion. Energetic particles associated with such defects provide a concrete candidate for the initiation species in our polymerization model of glass-forming liquids. Such interstitial defects are characterized by anisotropic long range dipole interactions that might explain the generic tendency of the mobile particle to self-assemble into strings, as in ordinary dipolar fluids.<sup>31</sup> These possibilities remain to be checked by refinements of our model.
- <sup>66</sup>A. S. Keys, L. O. Hedges, J. P. Garrahan, S. C. Glotzer, and D. Chandler, *Phys. Rev. X* **1**, 021013 (2011).
- <sup>67</sup>N. Giovambattista, S. V. Buldyrev, F. W. Starr, and H. E. Stanley, *Phys. Rev. E* **72**, 011202 (2005).
- <sup>68</sup>S. Sastry, P. G. Debenedetti, and F. H. Stillinger, *Nature* **393**, 554 (1998).
- <sup>69</sup>A. J. Rahedi, J. F. Douglas, and F. W. Starr, *J. Chem. Phys.* **128**, 024902 (2008).
- <sup>70</sup>J. F. Douglas, J. Dudowicz, and K. F. Freed, *J. Chem. Phys.* **125**, 144907 (2006).
- <sup>71</sup>Y. Gebremichael, T. B. Schröder, F. W. Starr, and S. C. Glotzer, *Phys. Rev. E* **64**, 051503 (2001).
- <sup>72</sup>W. Götz, *Liquids, Freezing and the Glass Transition* (North-Holland, Amsterdam, 1991), pp. 287–503.
- <sup>73</sup>U. Tracht, M. Wilhelm, A. Heuer, H. Feng, K. Schmidt-Rohr, and H. W. Spiess, *Phys. Rev. Lett.* **81**, 2727 (1998).
- <sup>74</sup>O. Yamamuro, I. Tsukushi, A. Lindqvist, S. Takahara, M. Ishikawa, and T. Matsuo, *J. Phys. Chem. B* **102**, 1605 (1998).
- <sup>75</sup>L. Hong, P. D. Gujrati, V. N. Novikov, and A. P. Sokolov, *J. Chem. Phys.* **131**, 194511 (2009).
- <sup>76</sup>D. Huang, D. M. Colucci, and G. B. McKenna, *J. Chem. Phys.* **116**, 3925 (2002).
- <sup>77</sup>H. Vogel, *Phys. Zeit* **23**, 645 (1921).
- <sup>78</sup>G. S. Fulcher, *J. Am. Ceram. Soc.* **8**, 339 (1925).
- <sup>79</sup>G. Tammann and W. Hesse, *Z. Anorg. Allg. Chem.* **156**, 245 (1926).
- <sup>80</sup>J. Zhao, S. L. Simon, and G. B. McKenna, *Nat. Commun.* **4**, 1783 (2013).
- <sup>81</sup>Q. Yan, T. S. Jain, and J. J. de Pablo, *Phys. Rev. Lett.* **92**, 235701 (2004).
- <sup>82</sup>G. P. Johari and J. Khouri, *J. Chem. Phys.* **134**, 034515 (2011).
- <sup>83</sup>G. Kohring, R. E. Shrock, and P. Wills, *Phys. Rev. Lett.* **57**, 1358 (1986).
- <sup>84</sup>J. Dudowicz, K. F. Freed, and J. F. Douglas, *Adv. Chem. Phys.* **137**, 125 (2008).
- <sup>85</sup>J. Dudowicz, K. F. Freed, and J. F. Douglas, *J. Chem. Phys.* **113**, 434 (2000).
- <sup>86</sup>H. Zhang, P. Kalvapalle, and J. F. Douglas, *J. Phys. Chem. B* **115**, 14068 (2011).
- <sup>87</sup>H. Zhang, D. J. Srolovitz, J. F. Douglas, and J. A. Warren, *Proc. Natl. Acad. Sci. U.S.A.* **106**, 7735 (2009).
- <sup>88</sup>K. H. Nagamanasa, S. Gokhale, R. Ganapathy, and A. K. Sood, *Proc. Natl. Acad. Sci. U.S.A.* **108**, 11323 (2011).
- <sup>89</sup>R. A. Riggelman, K. Yoshimoto, J. F. Douglas, and J. J. de Pablo, *Phys. Rev. Lett.* **97**, 045502 (2006).
- <sup>90</sup>Z. Gai, H. Yu, and W. Yang, *Phys. Rev. B* **53**, 13547 (1996).
- <sup>91</sup>E. R. Weeks, J. C. Crocker, A. C. Levitt, A. Schofield, and D. A. Weitz, *Science* **287**, 627 (2000).
- <sup>92</sup>R. Feynmann, *Progress in Low Temperature Physics* (Elsevier, 1955), Vol. I.
- <sup>93</sup>A. K. Nguyen and A. Sudbø, *Phys. Rev. B* **60**, 15307 (1999).
- <sup>94</sup>C. Dasgupta and B. I. Halperin, *Phys. Rev. Lett.* **47**, 1556 (1981).
- <sup>95</sup>A. J. Chorin, *Phys. Rev. Lett.* **60**, 1947 (1988).
- <sup>96</sup>R. Zwanzig, *Phys. Rev.* **156**, 190 (1967).
- <sup>97</sup>R. A. Riggelman, J. F. Douglas, and J. J. de Pablo, *Phys. Rev. E* **76**, 011504 (2007).
- <sup>98</sup>H. Zhang and J. F. Douglas, *Soft Matter* **9**, 1266 (2013).